

Improving the high temperature oxidation resistance of Ti-β21S by mechanical surface treatment

L. Lavisse^{a*}, A. Kanjer^a, K. Cheveau^a, V. Optasanu^a, P. Peyre^b, C. Gorny^b, M. François^c, A. Tidu^d, C. Schuman^d, F. Herbst^a, M. Saint-Jean^c, T. Montesin^a,
M. C. Marco de Lucas^a

^a Laboratoire Interdisciplinaire Carnot de Bourgogne (ICB), UMR 6303 CNRS-Université de Bourgogne Franche-Comté, Dijon, France;

^b Laboratoire PIMM, Ensam ParisTech, Paris, France;

^c Institut Charles Delaunay, UTT, Troyes, France;

^d LEM3, Université de Lorraine, CNRS, Arts et Métiers ParisTech, Metz, France;

^e IUT Chalon sur Saône, Université de Bourgogne, Chalon sur Saône, France

* Corresponding author: luc.lavisse@u-bourgogne.fr

Abstract

The improvement of the high temperature oxidation resistance of titanium alloys is currently a technological challenge. Mechanical surface treatments as shot-peening (SP) have shown their ability to improve the behaviour of pure zirconium and titanium. However, shot-peening treatments can induce a significant surface contamination. Laser shock peening (LSP) appears as a good alternative. Here, we have investigated the effect of SP and LSP treatments on the HT oxidation behavior of Ti-β21S. Samples treated by these methods have been compared to untreated ones for long exposures (3000 h) at 700 °C in dry air. The samples placed in a furnace at 700 °C were periodically extracted to be weighed. The results have been compared to that of pure commercial titanium (Ti-α) samples studied in the same conditions. The higher performances of the Ti-β21S alloy, and the beneficial effect of the SP treatment, and even more of the LSP one, on the HT oxidation resistance of Ti-β21S have been clearly shown. The effect of the mechanical treatments on the microstructure of the Ti-β21S samples and the changes induced by the long duration exposure at high temperature have been mainly studied by scanning electron microscopy combined with energy and wavelength dispersive spectrometry.

1. Introduction

The excellent combination of light-weight and good mechanical properties makes Ti alloys attractive for compressor section components in gas turbine engines [1]. Compared to Ni super alloys and steels, Titanium offers a potential weight savings in the order of 50%. However, the protection of titanium alloys against oxidation at high temperatures (HT), above 600 °C, is required to allow a wider use of Ti alloys at high operating temperatures in gas-turbine engines and other industrial components. At low temperatures, below 600 °C, Ti alloys show very good corrosion resistance thanks to the titanium dioxide passive surface layer. Above 600°C, the deterioration of the passivation layer and the oxide spallation lead to increasing oxidation. The result is an inward diffusion of oxygen under the oxidation layer and the formation of an oxygen-rich area in the metal, so-called the α-case area [2]. In the case of oxidation in air, the formation of nitrides at the interface between the oxide layer and the α-case area was discussed by Chaze and Coddet [3]. This nitride layer would slow down the oxygen diffusion and then induce a protection in terms of oxidation.

The development of efficient oxidation-resistant surface treatments and coatings for titanium alloys is necessary. Two main problems are usually encountered in the HT behavior of coatings for Ti alloys: i) interdiffusion between the coating and the bulk and ii) the breaking of the coating or the oxide layer. The main treatments developed for HT protection of titanium alloys are ion implantation [4], pack cementation coatings [5] and PVD ceramic coatings [6]. Mechanical surface treatments are less used for oxidation protection purposes, but are widely used to improve the mechanical surface properties as tribological [7] or fatigue behavior [8]. Recent works by Raceanu *et al.* [9] show a positive role of the mechanical treatments in the oxidation resistance of zirconium due to the large compressive stresses induced by the treatment underneath the surface. More recently, Kanjer *et al.* reported the beneficial effect of mechanical treatments on the oxidation resistance of pure titanium at high temperature in air [10-12].

In this work, we investigate the effect of two mechanical treatments, shot-peening (SP) and laser shock-peening (LSP), on the oxidation resistance of Ti-β21S alloy at 700 °C in air. Non-isothermal mass gain measurements were recorded for HT exposure during 3000 h. They showed a reduction of the oxidation rate compared to untreated samples. The cross-section of oxidized samples was studied by scanning electron microscopy coupled with electron microprobe analysis (EDS and WDS). The insertion of nitrogen and the segregation of different alloying elements as a consequence of the HT exposure was studied in this way. LSP appears here as the best treatment to improve the HT resistance of Ti-β21S.

2. Material and experiments

2.1 Material

Ti-β21S is an alloy from TIMET society. It contains β-stabilizing elements such as Mo 15.13 (wt. %), Nb 2.65, Fe 0.26, Si 0.2 and also some α-stabilizing elements such as Al 3.45, O 0.13, N 0.02 and C 0.013. Before the surface treatments, the samples were cut from 1.8 mm thick foils to obtain 25 x 25 x 1.8 mm³ plates. After the mechanical treatment, the samples devoted to thermal analysis were cut to a size of 8 x 10 x 1.8 mm³. In the following, the untreated samples will be named Tiβ-US, while the Tiβ-SP and Tiβ-LSP treated samples will be called SP and LSP.

2.2 Experiments

The mechanical surface treatments were performed using two different methods. The first one is shot peening by surface mechanical attrition treatment (SMAT) with WC balls of 2 mm. This method consists of vibrating WC balls in a closed chamber by using high-power ultrasound (with 20 kHz frequency). The balls projected on the sample surface induce large residual compressive stresses, strong plastic strains and a nano-structuration of the sub-surface of the material [13, 14]. The height of the chamber is 15 mm and the amplitude of vibration during the treatment is 12 μm. The samples were treated during 30 minutes on each face with reversing of the treated face each 10 minutes in order to keep bending deformations reasonable.

The second treatment studied here is the laser shock peening by short impulsions of a high intensity laser on the surface sample. The treatment was operated in water to increase the shock amplitude [15, 16]. An adhesive aluminum film is pasted on the surface of the sample to protect it against thermal effects or oxidation. The laser used here was a GAIA HP with a frequency of 0.5 Hz, a pulse duration of 7 ns, and laser irradiance of 9.1 GW/cm². Each laser impact generates a plasma plume over the target and the plasma extinction generates a shock wave into the target.

The surface roughness of untreated and treated samples was studied by using an optical profilometer VEECO WYCO NT 9100. Micro-hardness profiles were measured in cross section of the samples using a ZWICK/ROELL ZHVμ microhardness tester with a Vickers diamond pyramid indenter and a load of 0.5 N after treatments and 0.25 N for α-case depth determination. The load is applied during 10 s.

Before and after the oxidation experiments, the samples were studied by X-ray diffraction and micro-Raman spectroscopy. XRD patterns were obtained with a Bruker D8-A25 DISCOVER goniometer using Cu-K_α radiation.

Long-time HT oxidation experiments (3000 h) were carried out within a SETNAG furnace at 700 °C under synthetic dry air. The samples were extracted from the furnace once a week to be weighed. After this, around 1 h later, they were placed again in the furnace, which was maintained at 700 °C. Therefore, the treatment was not completely isothermal.

Before and after the oxidation experiments, the cross-section of the different samples was investigated by SEM in back-scattering electron mode (BSE) with a TESCAN VEGA 3 combined with an energy dispersive spectrometer (EDS).

3. Results and discussion

3.1 Effects of the mechanical treatments: characterizations before HT oxidation

SEM cross-section images and 3D-surface maps of Tiβ-US, Tiβ-SP and Tiβ-LSP samples are shown in Figure 1. The repetition of the impacts on the sample during SP treatments can generate large residual compressive stresses, plastic deformation and nano-structuration within a layer of several hundreds of micrometers under the surface of the material [13]. For Tiβ-SP samples, the SEM cross-section images clearly show the effect of the treatment in a layer about 100 μm thick underneath the surface. The grains display twinning and their size seems slightly smaller in this layer than at the material core. On the contrary, the effect of the LSP treatment is not limited to a top layer, but it is revealed by the appearance of twinning through the whole thickness of the sample.

Figure 1 shows quite a different surface topography for the three kinds of samples. Tiβ-US samples display parallel grooves due to the cold-rolling manufacture process. For Tiβ-SP samples, this effect is replaced by a rough surface due to the impact of the WC balls used for this treatment. The arithmetic averaged roughness value, R_a, is higher compared to untreated samples. The LSP treatment strongly reduces the surface grooves. The averaged roughness value, R_a is similar to untreated samples, but the total roughness value, R_t, is lower.

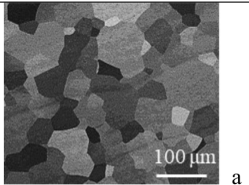
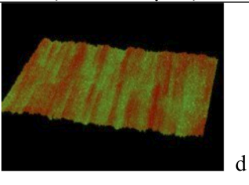
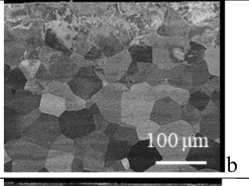
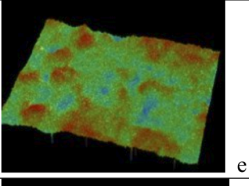
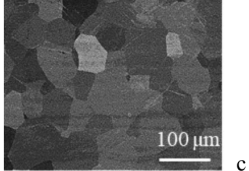
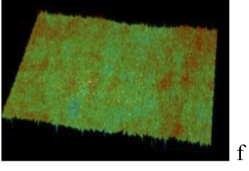
Samples	SEM – BSE	Surface maps (640 x 480 μm ²)	Roughness	
			Ra (μm)	Rt (μm)
US			0.4	6.4
SP			0.8	9.2
LSP			0.4	6.2

Figure 1 - (a,b,c) Cross-section SEM images (BSE mode) of Tiβ-US, Tiβ-SP and Tiβ-LSP samples. (d,e,f) 3D-surface maps obtained by using a VEECO WYKO NT 9100 VEECO WYKO NT9100 optical profilometer. The corresponding roughness values Ra and Rt are also given.

Micro-hardness in-depth profiles through the cross-section of untreated and treated samples are given in Figure 2. For the raw material (Tiβ-US), the in-depth hardness profile is nearly flat with a value of 325 HV. The profile of Tiβ-SP samples shows a strong hardness gradient from the core of the sample, where the hardness is the same of US samples, to the surface where a strong hardening of about 60 HV is observed. For Tiβ-LSP samples the hardening near the surface is negligible.

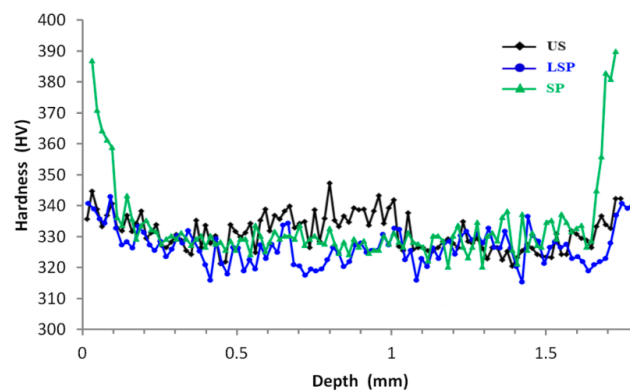


Figure 2 - Micro-hardness measurements of untreated and mechanically treated Ti-β21S samples.

XRD patterns of Tiβ-US, Tiβ-SP and Tiβ-LSP samples are displayed in Figure 3. They reveal a change in the crystallographic texture of titanium due to the surface treatments. This is shown by the decrease of absolute intensity of all the diffraction peaks after SP and LSP treatment. Some peaks have almost disappeared, as those of Ti-β (200) and Ti-β (200) reflections. The broadening of the diffraction peaks suggests a crystallite size reduction or an increase in lattice distortion (dislocations, twins, ...) also as

a consequence of the treatments. For Tiβ-SP samples, the contamination of the surface due to the WC balls used for the SP treatment is clearly seen in the XRD pattern which displays several peaks attributed to WC.

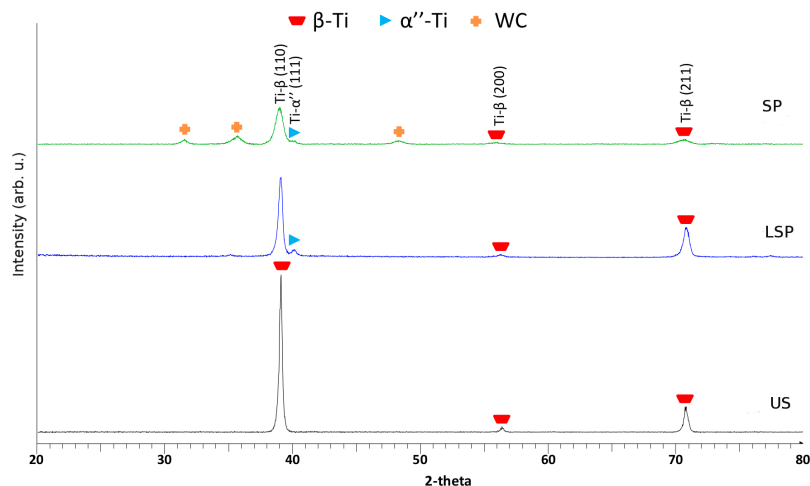


Figure 3: XRD patterns of untreated (US) and mechanically treated Ti-β21S samples.

3.2 Long-duration HT oxidation experiments

Figure 4 shows the variation of the mass gain for long-duration (3000 h) HT oxidation experiments. No spallation of the oxide layer was observed for any of the three kinds of samples. The total mass gain for Tiβ-US samples was 2.90 mg/cm². It was reduced to 1.82 mg/cm² for Tiβ-SP samples and it decreases to 1.16 mg/cm² for Tiβ-LSP samples. This is almost three times smaller than the mass gain of untreated samples. So, the beneficial effect of both SP and LSP treatments on the HT oxidation resistance of Ti-β21S is clearly demonstrated by the reduction of the mass gain after 3000 h at 700 °C.

As it was reported in previous works [11,12], in the case of commercially pure Ti-α untreated and SP treated samples studied in the same conditions showed spallation of the oxide layer after about 1700 h at 7000 °C. On the contrary, LSP treated Ti-α showed a homogeneous oxide layer, and a mass gain of 6.7 mg/cm² after 3000 h.

A kinetic oxidation law (Eq. 1) was used to fit the mass gain as a function of the time shown in Fig. 4:

$$\Delta m/S = (k.t)^{1/n} \quad (\text{Eq. 1})$$

where Δm is the mass variation, S the sample surface, t the time, k the oxidation constant and n the power index of the kinetic law.

For the three kinds of samples, the experimental curve can be fitted by Eq. (1) in the whole time range with a parameter close to 2, corresponding to a parabolic kinetic law, which is associated to a protective barrier [17,18]. The corresponding parabolic k_p oxidation constant is equal to $8.3 \times 10^{-13} \text{ g}^2.\text{cm}^{-4}.\text{s}^{-1}$ for Tiβ-US, $2.9 \times 10^{-13} \text{ g}^2.\text{cm}^{-4}.\text{s}^{-1}$ for Tiβ-SP and $1.3 \times 10^{-13} \text{ g}^2.\text{cm}^{-4}.\text{s}^{-1}$ for Tiβ-LSP.

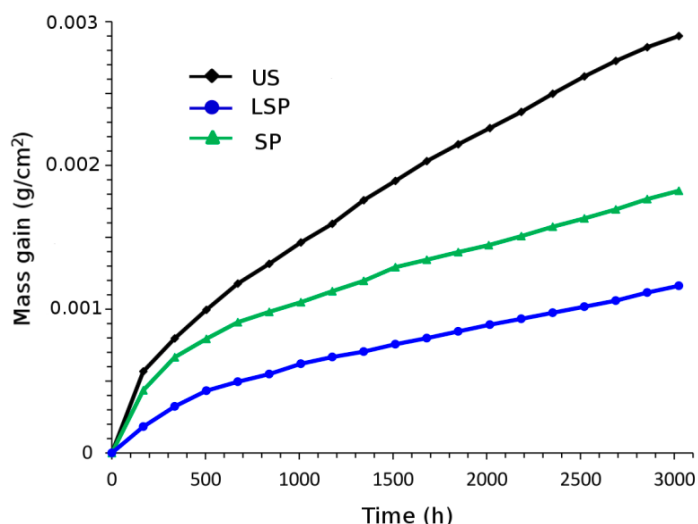


Figure 4 - Non-isothermal kinetic oxidation curves of Tiβ-US, Tiβ-SP and Tiβ-LSP samples for oxidation at 700 °C in dry air.

Figure 5 displays cross-section SEM-BSE images and EDS maps of Tiβ-US, Tiβ-SP and Tiβ-LSP samples after 3000 h at 700 °C in dry air. SEM images show the oxide layer with the highest thickness corresponds to the untreated sample. The oxide layer is about 10 μm in the image given in Fig. 6, but it is quite higher in other areas where the oxidation layer is stratified. This stratification of the oxidation layer was not observed for Tiβ-SP and Tiβ-LSP samples. The oxidation layer thickness was about 6 μm for Tiβ-SP, and 4 μm for Tiβ-LSP samples. Below the oxidation layer, SEM images also show a difference in the microstructure of the metal. The transformation of the titanium beta-phase (in light-grey in SEM images) into the α-phase (in dark grey) is mainly found at grain boundaries for US samples, while it is mainly observed inside the beta-phase grains for the SP treated sample. Finally, the transformation into α-phase is quite smaller in LSP samples. This supports the beneficial effect of the LSP treatment on the HT oxidation behavior of Ti-β21S.

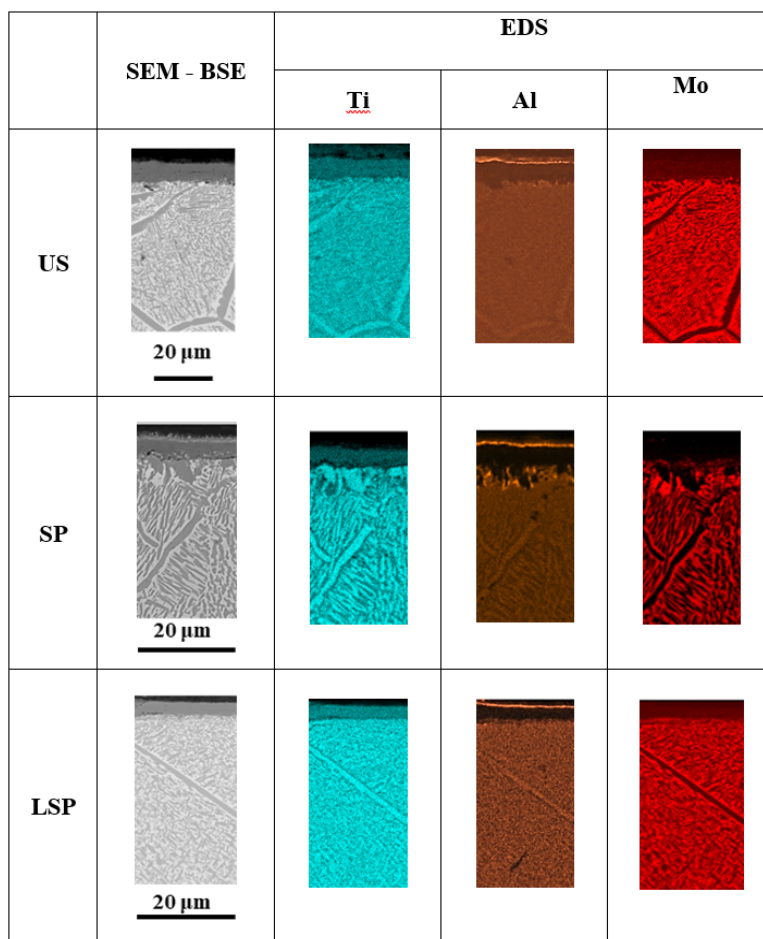


Figure 5 - On the left: Cross-section SEM images (in BSE mode) of Tiβ-US, Tiβ-SP and Tiβ-LSP samples after oxidation during 3000 h under dry air at 700 °C. The coating resin appears in black on top of the images. On the right: EDS maps showing the elemental distribution in the same areas zoomed in SEM images.

EDS maps (Fig. 5) show the spatial distribution of different elements (Ti, Al and Mo) in both the oxidation layer and the metal underneath. On top of all the samples, an external layer of alumina is observed as reported by Wallace *et al.* [19,20]. In the oxide layer, the EDS signal of molybdenum is very low, but it is clearly observed near the oxide-metal interface for the SP sample.

Below the oxide layer, the study of potential insertion of light elements, oxygen and nitrogen in the metal must be addressed by using other techniques as ion beam analysis. The insertion of nitrogen could play a role in the improvement of the HT oxidation resistance in air, as was reported by Chaze and Coddet for pure titanium and several binary alloys with aluminum, with chromium and with silicon [3].

Below the oxidation layer, the distribution of β-stabilizing elements (Mo) and α-stabilizing ones (Al) shows a different situation as regards the β to α-phase transformation as a function of the mechanical treatment used here. For Tiβ-US samples, Mo is almost absent in the grain boundaries which is the opposite for Al. This supports that the β to α-phase transformation mainly takes places in the grain boundaries for untreated samples. Moreover, molybdenum is also absent in large α-phase grains observed on top of the metal where the effects of the SP treatment were higher.

For Tiβ-LSP samples, the segregation of β and α-stabilizing elements is quite smaller which supports a smaller transformation of titanium into the α-phase, as reported by Behera *et al.* [21]. Moreover, this transformation is mainly observed inside the grain instead of the grain boundaries. Laser treatments can also induce a higher diffusion of aluminum and chromium in titanium alloys as reported by Hua *et al.* [22, 23]. However, the concentration of aluminum in the Ti-β21S alloy is low (3.45 wt. %), and maybe not enough to increase the oxidation resistance of titanium. Other hypothesis to explain the lower oxidation of Tiβ-LSP samples would be based on the texture induced by the treatment as it has been observed in preliminary studies. The induced texture could promote the epitaxial growth of the oxide scale and give rise to an adherent, compact and stoichiometric rutile layer. Further work is in progress.

4. Conclusions

This work has investigated the effect of two mechanical treatments, shot-peening (SP) and laser shock-peening (LSP), on the HT oxidation behavior of Ti-β21S. SP and LSP treated samples have been compared to untreated ones for long duration exposures (3000 h) at 700 °C in dry air. The higher HT oxidation resistance of the Ti-β21S alloy compared to commercially pure titanium Ti-α has been shown. Moreover, the beneficial effect of both SP and LSP treatments has been demonstrated for long exposure (3000 h) at 700 °C. The LSP treatment provided the best results reducing the mass gain by a factor 3 over 3000 h.

The analysis of Tiβ-SP and Tiβ-LSP samples before the oxidation experiments showed different effects on the microstructure of the samples. We found that the SP treatment induces important modifications, as twinning and grain size reduction at the surface of the samples down to about 100 μm. The effects of the LSP treatment are smaller, they were revealed by the appearance of twinning throughout the whole thickness of the sample. Moreover, the effect of the laser treatment on the crystallographic texture of titanium appears as a possibility to explain the higher oxidation resistance of LSP treated samples.

Besides oxidation, long exposure at high temperatures induced also a partial β- to α-phase transformation of titanium, which appears together with the segregation of the different β- and α-stabilizing alloying elements. It was observed that this transformation is lower in the case of Tiβ-LSP samples compared to untreated and SP treated samples. Moreover, it is mainly observed inside the grains, on the contrary of Tiβ-SP samples for which the transition is achieved mainly in the grain boundaries.

5. Acknowledgments

Authors acknowledge greatly Burgundy Regional Council (BRC) and the Agglomeration Council of Chalon City for their financial contribution in SEM at Chalon sur Saône.

6. References

- [1] I. Inagaki, T. Takechi, Y. Shirai, N. Ariyasu, Nippon Steel & Sumitomo Metal Technical Report No. 106 (2014)
- [2] J. Stringer, *Acta metallurgica* 8 (1960)
- [3] A. M. Chaze, C. Coddet, *Journal of the less common metals* 124 (1986) 73-84.
- [4] I. Gurappa, D. Manova, J.W. Gerlach, S. Mandl, B. Raushenbach, *Surf. Coat. Technol.* 201 (2006) 3536-3546
- [5] D. K. Das, S. P. Trivedi, *Mat. Sci Eng.* 367 (2004) 225-233
- [6] A. Ebach-Stahl, C. Eilers, N. Laska, *Surf. Coating Technol.* 223 (2013) 24-31
- [7] D. Wei, P. Zhang, Z. Yao, J. Zhou, X. Wei, P. Zhou, *Surf. Coat. Technol.* 204 (2012) 2343-2352
- [8] M. C. Marco de Lucas, L. Lavissee, G. Pillon, *Trib. Int.* 41 (2008) 985-991
- [9] L. Raceanu, V. Optasanu, T. Montesin, G. Montay, M. François, *Oxidation of Metal* 79 (2013) 135-145
- [10] A. Kanjer, V. Optasanu, L. Lavissee, and al *Oxid. Met.* 87 (2017) 1–13
- [11] A. Kanjer, L. Lavissee, V. Optasanu, & al., *Surf. Coat. Technol.*, 326A (2017) 146-155
- [12] A. Kanjer, V. Optasanu, M.C. Marco de Lucas, and al *Surf. Coat. Technol* 343 (2018) 93-100
- [13] M. Micoulaut, S. Mechkov, D. Retraint, P. Viot and M. François, *Granular Matter*, 9 (2005) 25
- [14] K.Y. Zhu, A. Vassel, F. Brisset, K. Ju and J. Lu, *Acta Materialia*, 52 (2004) 4101
- [15] P. Peyre, L. Berthe, V. Vignal, I. Popa and T. Baudin, *Journal of Physics*, 45 (2012) 335304
- [16] P. Peyre, C. Carboni, P. Forget, G. Beranger, C. Lemaître, D. Stuart, *J. of Mater. Sci.*, 42, (2007) 6866
- [17] H. E. Evans, *International Materials Reviews*, 40 (1995) 1
- [18] X. Guangjun, Y. Gaiying, Z. Jing, P. Yiqun, *Rare Metals*, 18 (1999)
- [19] T. A. Wallace, R. K. Clark, K.E. Wiedemann, *NASA Technical Memorandum, World Conference on Titanium, San Diego, 1992.*
- [20] T. A. Wallace, R. K. Clark, K. E. Wiedmann, *Mater. Sci.* (1993).
- [21] A. Behera, S. Nag, K. Mahdak, H. Mohseni, J. Tiley, R. Banerjee, *J. Mat. Sci.* 48 (2013) 6700-6706.
- [22] Y. Hua, Y. Bai, Y. Ye, Q. Xue, H. Liu, R. Chen, K. Chen, *Appl. Surf. Sci.* 283, (2013).p 775-780,
- [23] Y. Hua, Z. Rong, Y. Ye, K. Chen, R. Chen, Q. Xue, H. Liu, *Appl. Surf. Sci.* 330, (2015) 439-444.